Kinetic Modeling of Ethylene−Norbornene Copolymerization Using Homogeneous Metallocene Catalysts

Seung Young Park and Kyu Yong Choi*

Department of Chemical Engineering, University of Maryland, College Park, Maryland 20742

Kwang Ho Song and Boong Goon Jeong

LG Chem Research Park, 104-1 Moonji-dong, Yusong-gu, Taejon, 305-380 Korea

Received January 28, 2003; Revised Manuscript Received March 3, 2003

ABSTRACT: The kinetics of ethylene−norbornene copolymerization to cyclic olefin copolymer has been investigated using homogeneous *rac*-Et(1-indenyl)$_2$ZrCl$_2$/methylaluminoxane catalyst in toluene at 70 °C for norbornene/ethylene mole ratios in the range of 3−55. It is shown that the catalyst is ineffective for the homopolymerization of norbornene, but the catalyst activity for the insertion of norbornene into a growing polymer chain increases dramatically in the presence of ethylene. A terminal model has been developed to quantify the kinetic behavior of the copolymerization process, but it was found inadequate to represent the copolymerization kinetics for a broad range of polymerization conditions. To overcome the limitations of the terminal model we developed a penultimate model and excellent agreement between the experimental data and model calculations has been obtained. In particular, it is shown that the penultimate model accurately predicts the effect of bulk phase norbornene concentrations on the polymerization rate.

Introduction

Cyclic olefin copolymer (COC) is an amorphous thermoplastic polymer that can be synthesized without ring opening by addition polymerization mechanism using homogeneous metallocene catalysts. Among several cyclic olefin copolymers, the copolymer of ethylene and norbornene is one of the most promising new industrial thermoplastic polymers with its high glass transition temperature (T_g), excellent moisture barrier properties, chemical resistance, and optical clarity. Ethylene−norbornene copolymer (ENC) is very attractive as a novel substrate material for high-density data storage devices, packaging, and optical/biomedical applications. One of the interesting characteristics of ENC is that its glass transition temperature can be varied from about 20 to 260 °C by varying the norbornene content in the copolymer (10−80 mol %) and its microstructure.

The synthesis of ethylene−norbornene copolymer has been studied by many workers in the past several years, notably by Kaminsky and co-workers,[1−4] Bergström et al.,[5,6] and Ruchatz and Fink[7] using various types of homogeneous metallocene catalysts. It is interesting to note that many metallocene catalysts that are effective for ethylene polymerization are not effective for the homopolymerization of norbornene. The molecular modeling study by Bergström et al.[5] indicates that the insertion of three consecutive norbornene units is sterically very unlikely because there is not enough room at the active site for three norbornene units to be inserted in a row. However, the catalytic activity for norbornene polymerization increases significantly when norbornene is copolymerized with ethylene, making the incorporation of a large amount of norbornene into the copolymer possible. It is believed that the steric hindrance for the insertion of norbornene might be significantly reduced when ethylene is the last inserted monomer in a growing chain.[7] From ^{13}C NMR analysis at tetrad level, Tritto et al.[12] show that a significant amount of norbornene belonging to norbornene triads has been obtained using metallocenes with C_2 symmetry. Kaminsky and Knoll[3] report that the C_s-symmetric catalysts have better steric conditions for insertion of bulky norbornene than the C_2-symmetric catalysts. It is also interesting to point out that when ethylene is copolymerized with norbornene in a solvent such as toluene, the polymerization proceeds homogeneously because the copolymer is completely soluble in toluene at high norbornene content in the copolymer.

Ethylene−norbornene copolymer is also known to have a complex microstructure that depends on the nature of catalyst and the polymerization conditions.[7−13] For example, when norbornene content in the copolymer is small (less than 6 mol %), most of the norbornene units are present as isolated units with random sequence distribution.[14] The crystallinity of ENC decreases as the amount of norbornene increases. The copolymer becomes amorphous at norbornene content larger than about 14 mol %. For the copolymer containing more than 45 mol % norbornene, micronorbornene blocks of varying length (diads, triads) can be formed as confirmed by ^{13}C NMR spectroscopy.[8,10,14,15] But the presence of longer norbornene microblocks is quite difficult to confirm by current ^{13}C NMR technique. Theoretically the insertion of bulky norbornene into C-transition metal bond can take place in exo, endo, and exo−endo configurtions, but the exo-configuration is believed to be the predominant way of norbornene insertion.[14]

Some important properties of ethylene−norbornene copolymer are influenced by its microstructure. For example, the glass transition temperature of the ethylene−norbornene copolymer depends not only on the overall norbornene content but also on the microstruc-

* To whom correspondence should be addressed. E-mail: choi@eng.umd.edu. Telephone: (301) 405-1907. Fax: (301) 405-0523.

10.1021/ma034115+ CCC: $25.00
Published on Web 04/15/2003

ture of the copolymer.[13,16] The alternating and block sequences of norbornene in the copolymer make the polymer stiffer and T_g higher.[14] The ethylene−norbornene copolymers with similar compositions but different microstructures can have significantly different glass transition temperatures; the glass transition temperature of the stereoregular alternating copolymer is lower than the random copolymer.[16] Harrington and Crowther[16] also show that the decay of the elastic moduli in the stereoregular copolymer has a shallow slope above its glass transition temperature compared to the random copolymer of similar norbornene content. Therefore, it is of practical importance to understand how the copolymer properties are influenced by catalyst and polymerization conditions.

Although there are many reports on the synthesis of ethylene−norbornene copolymer and the characterization of its microstructure, very few report the kinetic analysis of metallocene catalyzed ethylene−norbornene copolymerization processes.[7,12,15,17] To date, the most comprehensive analysis of ethylene−norbornene copolymerization kinetics is the work by Ruchatz and Fink[7] who used [(isopropylidene)(η^5-inden-1-ylidene-η^5-cyclopentadienyl)]$ZrCl_2$/methylaluminoxane (MAO) catalyst at 70 °C for norbornene/ethylene mole ratio up to 25. Although no kinetic model was developed, their experimental work provides many interesting insights into the kinetics of ethylene−norbornene copolymerization. For example, they show that the ethylene polymerization rate increases linearly up to a certain ethylene concentration, but further increase in the bulk phase ethylene concentration causes no further increase in the ethylene polymerization rate. Also, their experimental data show that the norbornene polymerization rate passes through a maximum as bulk phase norbornene concentration is varied: norbornene polymerization rate increases as bulk phase norbornene/ethylene ([NB]/[E]) mole ratio is increased to about 0.8 but the rate decreases with further increase in the bulk phase [NB]/[E] mole ratio. They attributed the rate decrease at high norbornene concentrations to steric effects. Another modeling work to be noted is by Tritto and co-workers:[12,15] they used the first-order and second-order Markovian statistical models to analyze the sequence length distribution of ethylene−norbornene copolymers for various types of metallocene catalysts.

In view of the fact that the copolymer properties are strongly influenced by catalyst and reaction variables, it is necessary to have available a kinetic model for the quantitative analysis of the reaction kinetics and for the design of more efficient copolymerization processes. A good kinetic model is also needed to develop deeper insights into the copolymerization kinetics. In this work, we investigate the solution copolymerization kinetics through modeling and experimentation with C_2-symmetric *rac*-Et(1-indenyl)$_2ZrCl_2$ catalyst with MAO. In particular, we extend the first-order Markovian model (terminal model) we developed earlier[17] and propose a new model to overcome the limitations of the terminal model.

Experimental Section

Ethylene−norbornene copolymerization experiments were carried out at 70 °C using a 500 mL high-pressure stainless steel jacketed reactor equipped with a stirrer. *rac*-Et(1-indenyl)$_2ZrCl_2$ catalyst (Boulder Scientific) and modified methyl aluminoxane (MMAO type 3A, Akzo Nobel) were used without further purification. Norbornene (Aldrich) was dissolved in purified toluene and the solution was stored in a flask containing molecular sieve pellets for moisture removal. A desired amount of catalyst was weighed and placed into a stainless steel catalyst injection assembly under argon atmosphere in a glovebox. In all the experiments, MAO/Zr mole ratio was kept constant at 4000. The reactor was first charged with a known amount of toluene. Then, the reactor temperature was raised to the desired reaction temperature by circulating hot water in the reactor jacket. Purified ethylene gas was supplied to the reactor until toluene was saturated with dissolved ethylene. The polymerization was then started by the injection of catalyst solution. The reactor pressure was kept constant during the polymerization by controlling the ethylene addition rate. The reaction temperature, pressure, and ethylene flow rate were monitored and recorded through a data acquisition system. A small amount of reaction sample was taken during the polymerization and poured into a beaker containing a large amount of acetone. The precipitated polymer was washed using acidified methanol and washed again with fresh acetone before drying in a vacuum oven for more than 15 h. The polymerization was stopped by venting the reactor and the reaction mixture was discharged into a container filled with acetone. The glass transition temperature (T_g) was measured by differential scanning calorimetry (DSC, TA Instrument) and the copolymer composition was measured by ^{13}C NMR spectroscopy (500 MHz, Bruker).

Kinetic Modeling

One of the most important requirements for a kinetic model for ethylene−norbornene copolymerization is to have the ability of predicting the polymerization rate and copolymer properties (e.g., overall copolymer composition, sequence length distribution, molecular weight, etc.) for a broad range of polymerization conditions. To represent the copolymerization kinetics, the reactivity ratios are first determined but a dynamic model needs to be developed to calculate the polymerization rate. Also, the relevant kinetic rate constants must be determined from experimental data. In this work, we limit the goal of our property modeling to the prediction of overall copolymer composition that has the most important influence on the copolymer's glass transition temperature. To model the binary copolymerization process, let us first consider a simple terminal model.

Terminal Model. A terminal model is widely used for the modeling of Ziegler−Natta and metallocene catalyzed olefin copolymerization processes. The basic premise in the terminal model is that only the last inserted monomer unit at the active catalytic site is assumed to influence the propagation reaction. For the modeling of ethylene−norbornene copolymerization using the terminal model, we assume that the formation of active centers and chain initiation reaction are rapid and instantaneous. Then, the copolymer composition is determined by the four propagation reactions

$$M_1^* + M_1 \xrightarrow{k_{11}} M_1^* \quad (1)$$

$$M_1^* + M_2 \xrightarrow{k_{12}} M_2^* \quad (2)$$

$$M_2^* + M_1 \xrightarrow{k_{21}} M_1^* \quad (3)$$

$$M_2^* + M_2 \xrightarrow{k_{22}} M_2^* \quad (4)$$

where M_1 is ethylene (E), M_2 is norbornene (NB), and M_1^* and M_2^* are the growing polymer chains with M_1

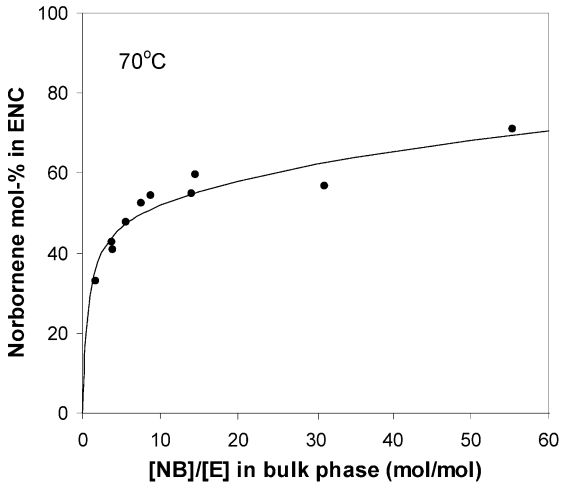

Figure 1. Copolymer composition curve at 70 °C with *rac*-Et(1-indenyl)$_2$ZrCl$_2$/MAO catalyst.

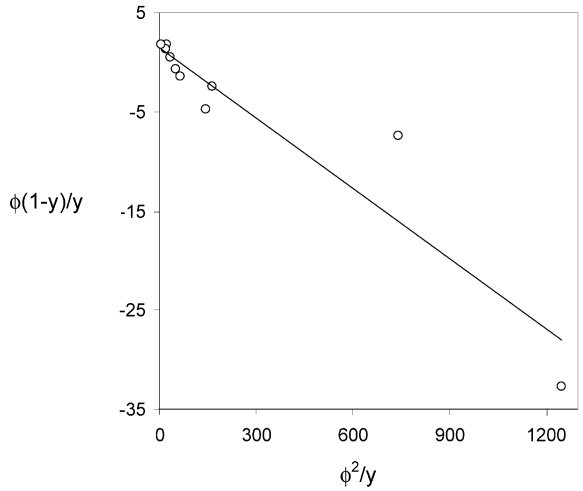

Figure 2. Fineman−Ross plot of ethylene−norbornene copolymerization data at 70 °C.

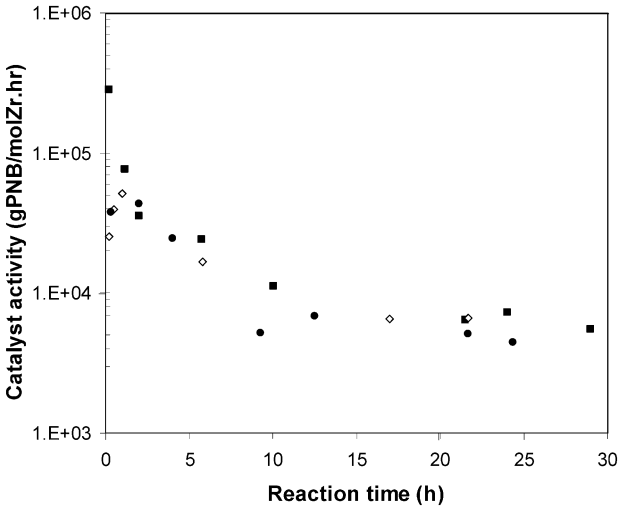

Figure 3. Catalyst activity in norbornene homopolymerization at 70 °C: (■) 5.94 × 10^{-7} mol-Zr; (◊) 1.36 × 10^{-6} mol-Zr; (●) 1.89 × 10^{-6} mol-Zr.

and M_2 as the last inserted monomer, respectively (i.e., M_1^* = polymer−M_1−Zr, M_2^* = polymer−M_2−Zr). The reactivity ratios are defined as $r_1 = k_{11}/k_{12}$ and $r_2 = k_{22}/k_{21}$. By applying the quasi-steady-state assumption to live polymers (M_1^* and M_2^*), we can derive the following well-known copolymer composition equation

$$\left(\frac{M_2}{M_1}\right)_p = \frac{M_2}{M_1}\frac{\left(1 + r_2\frac{M_2}{M_1}\right)}{\left(r_1 + \frac{M_2}{M_1}\right)} \tag{5}$$

where $(M_2/M_1)_p$ and M_2/M_1 are the norbornene/ethylene mole ratios ([NB]/[E]) in the polymer and the bulk reaction phases, respectively. Notice that copolymer composition is determined only by the monomer mole ratio and the reactivity ratios.

In a semibatch copolymerization experiment, ethylene concentration can be kept constant in the liquid phase by adding ethylene to the reactor to maintain the total pressure constant. Keeping the norbornene concentration (or [NB]/[E] mole ratio) constant in the reactor is not easy unless the exact amount of norbornene is added to the reactor to keep the monomer mole ratio constant during the polymerization. In practice, it is very difficult to do so. Hence, semibatch copolymerization experiment is carried out to low norbornene conversion to minimize the composition drift effect. In our experimental work, the copolymerization data taken at 10 min of reaction time are used for the kinetic analysis. The norbornene content in the copolymer can be best estimated from independent ^{13}C NMR experiments. In our study, the copolymer composition (i.e., norbornene content in mol %) is estimated using a T_g−composition correlation calibrated from the ^{13}C NMR data (T_g (°C) = 3.3751 X_{NB} − 41.4; X_{NB} = norbornene mol %).[18] It should be noted that the correlation used here does not take into account the effect of copolymer microstructure represented by the monomer sequence length distribution. It is because such effects have not been firmly quantified as reported in the literature.[13,16]

Figure 1 shows the experimentally measured norbornene mol % in the copolymer (symbols) at different [NB]/[E] mole ratios in the bulk liquid phase at 70 °C. Note that the experimental data shown in Figure 1 cover the norbornene concentration in the bulk liquid-phase ranging from 79.6 mol % ([NB]/[E] = 3.9) to 98.2 mol % ([NB]/[E] = 55.3). The corresponding range of T_g of the copolymers is 96−198 °C. The following Fineman−Ross equation is used to determine the reactivity ratios:

$$\frac{(1-y)}{y}\phi = r_1 - r_2\frac{\phi^2}{y} \tag{6}$$

where $y = (M_2/M_1)_p$ and $\phi = M_2/M_1$.

The reactivity ratios obtained from the Fineman−Ross plot in Figure 2 are: $r_1 = 1.47$, $r_2 = 0.024$. These values are very similar to those reported in the literature.[15,19] The very small value of r_2 indicates that the insertion of bulky norbornene into the Zr−norbornene bond is much more difficult than the insertion of ethylene into the Zr−norbornene bond. It is also interesting to note from the r_1 value that the rate constant for norbornene insertion into an M_1^* site (k_{12}) is surprisingly large: k_{12} is 67% of the ethylene homopolymerization rate constant (k_{11}). In other words, when ethylene is the last inserted unit in a growing polymer chain, steric effect is not quite strong for the insertion

of ethylene and norbornene, albeit with slightly larger steric effect for norbornene insertion. The solid line in Figure 1 shows the calculated copolymer composition using these reactivity ratios. It should be pointed out that the data shown in Figure 1 represent relatively high concentrations of norbornene in the liquid phase (e.g., [NB]/[E] = 2 corresponds to 67 mol % norbornene). The concentration of ethylene dissolved in the liquid phase at a given temperature is calculated using the Henry−Gesetz equation.[18] In our experiments, we found that the solubility of ethylene in toluene was little affected by the presence of norbornene. Figure 1 indicates that norbornene content increases rapidly with an increase in [NB]/[E] mole ratio in the liquid phase up to about 10 (about 90 NB mol %). As the bulk phase norbornene concentration increases further, the increase in the norbornene content in the copolymer phase increases only slightly. It is interesting to observe in Figure 1 that the asymptotic value of norbornene contents in the polymer is about 65−70 mol %, suggesting that the average sequence length of norbornene in the copolymer is about 2.

In addition to the reactivity ratios, the individual rate constants in eqs 1−4 need to be known to calculate the polymerization rate and copolymer yield. The rate equations for ethylene and norbornene take the following form:

$$\frac{dM_1}{dt} = -(k_{11}M_1^* + k_{21}M_2^*)M_1 \quad (7)$$

$$\frac{dM_2}{dt} = -(k_{12}M_1^* + k_{22}M_2^*)M_2 \quad (8)$$

If we assume that $C^* \approx M_1^* + M_2^*$ (C^* = total catalyst site concentration), the live polymer concentrations are expressed as

$$M_1^* = \frac{1}{\left(1 + \frac{k_{12}}{k_{21}}\frac{M_2}{M_1}\right)}C^*, \quad M_2^* = \frac{1}{\left(1 + \frac{k_{21}}{k_{12}}\frac{M_1}{M_2}\right)}C^* \quad (9)$$

Then the overall copolymerization rate is given by

$$R_p = R_{p1} + R_{p2} = \left[\frac{k_{11}}{1 + \frac{k_{12}}{k_{21}}\frac{M_2}{M_1}} + \frac{k_{21}}{1 + \frac{k_{21}}{k_{12}}\frac{M_1}{M_2}}\right]C^*M_1 + \left[\frac{k_{12}}{1 + \frac{k_{12}}{k_{21}}\frac{M_2}{M_1}} + \frac{k_{22}}{1 + \frac{k_{21}}{k_{12}}\frac{M_1}{M_2}}\right]C^*M_2 \quad (10)$$

where R_{p1} and R_{p2} are the ethylene and norbornene polymerization rates, respectively.

The cross-propagation rate constants (k_{12}, k_{21}) can be estimated from the reactivity ratios and the homopolymerization rate constants (k_{11}, k_{22}). We carried out ethylene homopolymerization experiments and the following homopolymerization rate constant was obtained at 70 °C: $k_{11} = 1.67 \times 10^7$ (L/mol·h). The observed ethylene homopolymerization rate was 3.52×10^7 g/mol-Zr·h. To estimate k_{22}, norbornene homopolymerization experiments were also carried out at three different catalyst concentrations and Figure 3 shows the polymerization rate profiles. As mentioned earlier, *rac*-Et(1-indenyl)$_2$ZrCl$_2$/MAO catalyst system has been known as a poor catalyst for norbornene homopolymerization. Figure 3 shows that the norbornene polymerization rate is indeed far smaller than the ethylene polymerization rate (e.g., $R_{p1} = 3.52 \times 10^7$ g/mol-Zr·h at 70 °C). Also, notice that the catalyst activity is almost independent of catalyst concentration, suggesting that the experimental results are quite consistent. The polymerization rate data also show that catalyst activity declines over the first 10 h reaction periods and then levels off. Since ethylene−norbornene copolymerization experiments lasted for 10 min in our kinetic study, the long-term catalyst deactivation effect for norbornene homopolymerization can be ignored. Thus, k_{22} value was determined by taking the average of the k_{22} values obtained from the initial rate data in the three experimental runs. The norbornene homopolymerization rate constant obtained is $k_{22} = 1.56 \times 10^2$ L/mol·h. Note that the norbornene homopolymerization rate constant is about 5 orders of magnitude smaller than the ethylene homopolymerization rate constant. The calculated cross-propagation rate constants are as follows: $k_{12} = 1.136 \times 10^7$ L/mol·h and $k_{21} = 6.5 \times 10^3$ L/mol·h. It is interesting to notice that $k_{21}/k_{11} = 0.00039$: ethylene is very difficult to be inserted into the Zr−norbornene bond because of steric hindrance of the bulky norbornene. Also, $k_{12}/k_{22} = 7.28 \times 10^4$: norbornene can be readily inserted into Zr−ethylene bond. Qualitatively similar results were reported by Ruchatz and Fink[7] with [(Isopropylidene)(η^5-inden-1-ylidene-η^5-cyclopentadienyl)]-ZrCl$_2$/MAO catalyst system.

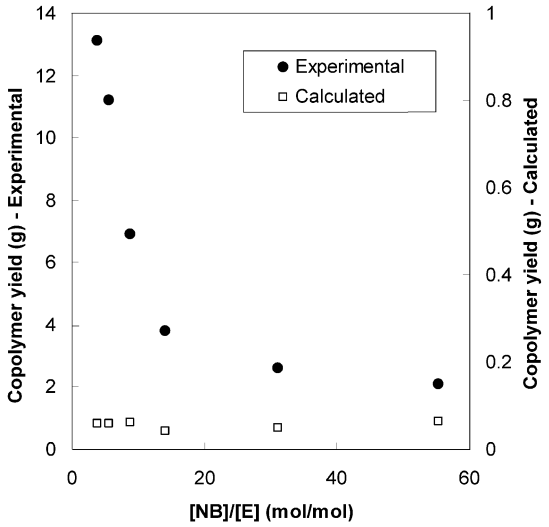

Figure 4. Copolymer yields: experimental data and terminal model calculations.

With these rate constants, the polymerization rate equations have been solved to calculate the copolymer yields for different bulk phase [NB]/[E] mole ratios and the results are shown in Figure 4 (reaction time = 10 min). Surprisingly, the calculated copolymer yields are significantly lower than the experimentally measured. To understand why the model-calculated copolymer yields are so low, let us first take a look at the calculated mole ratio of the propagating centers, $M_2^*/M_1^* = (k_{12}/k_{21})(M_2/M_1) = (1.75 \times 10^3)(M_2/M_1) \gg 1$. Since $M_2/M_1 > 1$ in all our experiments, we can state that as soon as the polymerization starts practically almost every cata-

lytic site is taken by norbornene and becomes the M_2^* site. Recall that the norbornene homopolymerization rate constant k_{22} is 5 orders of magnitude smaller than the ethylene homopolymerization rate constant. Therefore, once the Zr site is taken by norbornene, the subsequent insertion of either ethylene or norbornene is very difficult (e.g., $k_{21} \ll k_{11}$, $k_{22} \ll k_{12}$). In other words, the norbornene sites (M_2^*) are practically blocking the entire polymerization reaction and very little monomers are polymerized.

In contrary to this terminal model results, however, the experimental data show that both ethylene and norbornene are polymerized at higher reaction rates than the model predicted. We thought that the extremely small value of k_{22} determined from our experimental data might have caused such low polymerization rates. To see if the polymerization rates can be increased by using larger norbornene homopolymerization rate constant (k_{22}), the polymerization rates have been recalculated using the k_{22} values that are 200−500 times larger than the experimentally determined (both r_1 and r_2 values were held constant). The model-calculated norbornene polymerization rates are shown in Figure 5. We find that the calculated polymerization rates approach the experimental values as k_{22} is increased by 200−500 times. But there is a problem: Although the calculated polymerization rates approach the experimental values, the model-calculated dependence of norbornene polymerization rate on the bulk phase norbornene concentration contradicts the experimental observations. While the model predicts increasing norbornene polymerization rate with increasing bulk phase norbornene concentration, the experimental data show the opposite trends.

The monotonic increase in norbornene polymerization rate with increasing bulk phase norbornene concentration can be verified by analyzing the norbornene polymerization rate equation derived from the terminal model. The following eqation, eq 11, is the derivative of norbornene polymerization rate with bulk phase norbornene concentration:

$$\frac{d(R_{p2}/C^*M_1)}{d(M_2/M_1)} = \frac{1}{\left(1+\frac{k_{12}M_2}{k_{21}M_1}\right)^2}\left\{k_{12} + 2\frac{k_{22}k_{12}}{k_{21}}\frac{M_2}{M_1} + k_{22}\left(\frac{k_{12}}{k_{21}}\frac{M_2}{M_1}\right)^2\right\} > 0 \quad (11)$$

Indeed, eq 11 shows that norbornene polymerization rate always increases with bulk phase norbornene concentration. Since this terminal model calculation results do not agree with actual experimental results, we conclude that the terminal model is inadequate to represent the kinetics of ethylene and norbornene copolymerization with the catalyst used in this study.

Penultimate Model. From the monomer sequence distribution analysis by ^{13}C NMR spectroscopy, Tritto and co-workers[15] suggest that penultimate ethylene or norbornene unit exerts an influence on the reactivity of the propagating $Zr-M_1^*$ or $Zr-M_2^*$ species. To better account for the steric effect of norbornene, we consider a penultimate model. The penultimate model for a binary copolymerization process is represented as follows:

$$M_1M_1^* + M_1 \xrightarrow{k_{111}} M_1M_1^* \quad (12.1)$$

$$M_1M_1^* + M_2 \xrightarrow{k_{112}} M_1M_2^* \quad (12.2)$$

$$M_2M_1^* + M_1 \xrightarrow{k_{211}} M_1M_1^* \quad (12.3)$$

$$M_2M_1^* + M_2 \xrightarrow{k_{212}} M_1M_2^* \quad (12.4)$$

$$M_1M_2^* + M_1 \xrightarrow{k_{121}} M_2M_1^* \quad (12.5)$$

$$M_1M_2^* + M_2 \xrightarrow{k_{122}} M_2M_2^* \quad (12.6)$$

$$M_2M_2^* + M_1 \xrightarrow{k_{221}} M_2M_1^* \quad (12.7)$$

$$M_2M_2^* + M_2 \xrightarrow{k_{222}} M_2M_2^* \quad (12.8)$$

where $M_iM_j^*$ represents the growing polymer chain with monomer M_j as the last inserted unit and M_i as the penultimate unit (i.e., polymer$-M_iM_j-$Zr). The reactivity ratios are defined as

$$r_{11} = \frac{k_{111}}{k_{112}}, \quad r_{21} = \frac{k_{211}}{k_{212}}, \quad r_{12} = \frac{k_{122}}{k_{121}}, \quad r_{22} = \frac{k_{222}}{k_{221}} \quad (13.1)$$

The following additional reactivity ratios can also be defined as follows:

$$s_1 = \frac{k_{211}}{k_{111}}, \; s_2 = \frac{k_{122}}{k_{222}} \quad (13.2)$$

The rate equations for ethylene, norbornene, and propagating centers take the following form:

$$\frac{dM_1}{dt} = -(k_{111}M_{11}^* + k_{211}M_{21}^* + k_{121}M_{12}^* + k_{221}M_{22}^*)M_1 \quad (14)$$

$$\frac{dM_2}{dt} = -(k_{112}M_{11}^* + k_{212}M_{21}^* + k_{122}M_{12}^* + k_{222}M_{22}^*)M_2 \quad (15)$$

$$\frac{dM_{11}^*}{dt} = -k_{112}M_{11}^*M_2 + k_{211}M_{21}^*M_1 \quad (16)$$

$$\frac{dM_{21}^*}{dt} = k_{121}M_{12}^*M_1 + k_{221}M_{22}^*M_1 - k_{211}M_{21}^*M_1 - k_{212}M_{21}^*M_2 \quad (17)$$

$$\frac{dM_{12}^*}{dt} = k_{112}M_{11}^*M_2 + k_{212}M_{21}^*M_2 - k_{121}M_{12}^*M_1 - k_{122}M_{12}^*M_2 \quad (18)$$

$$\frac{dM_{22}^*}{dt} = k_{122}M_{12}^*M_2 - k_{221}M_{22}^*M_1 \quad (19)$$

In the above equations, M_{ij}^* represents $M_iM_j^*$ (polymer$-M_iM_j-$Zr). By application of the quasi-steady-state assumption to live polymers, the active site concentrations are derived:

$$M_{11}^* = \beta C^* \tag{20}$$

$$M_{21}^* = \beta \frac{k_{112}}{k_{211}} \frac{M_2}{M_1} C^* \tag{21}$$

$$M_{12}^* = \beta \frac{k_{112}}{k_{121}} \frac{M_2}{M_1} \frac{1 + \frac{1}{r_{21}} \frac{M_2}{M_1}}{1 + r_{12} \frac{M_2}{M_1}} C^* \tag{22}$$

$$M_{22}^* = \beta \frac{k_{112}}{k_{221}} r_{12} \left(\frac{M_2}{M_1}\right)^2 \frac{1 + \frac{1}{r_{21}} \frac{M_2}{M_1}}{1 + r_{12} \frac{M_2}{M_1}} C^* \tag{23}$$

where

$$\beta \triangleq \left(1 + \frac{k_{112}}{k_{211}} \frac{M_2}{M_1} + \frac{k_{112}}{k_{121}} \frac{M_2}{M_1} \left(1 + \frac{1}{r_{21}} \frac{M_2}{M_1}\right) \times \frac{\left(1 + \frac{k_{121}}{k_{221}} r_{12} \frac{M_2}{M_1}\right)}{1 + r_{12} \frac{M_2}{M_1}}\right)^{-1} \tag{24}$$

In deriving the above equations, we also assumed no loss of catalytic sites:

$$C^* \approx M_{11}^* + M_{21}^* + M_{12}^* + M_{22}^*$$

Then the copolymer composition equation is derived for the penultimate model as follows:

$$\left(\frac{M_2}{M_1}\right)_p = \left(\frac{M_2}{M_1}\right) \frac{1 + r_{12} \frac{M_2}{M_1} \left(\frac{1 + r_{22} \frac{M_2}{M_1}}{1 + r_{12} \frac{M_2}{M_1}}\right)}{r_{11} \left(\frac{1 + \frac{1}{r_{11}} \frac{M_2}{M_1}}{1 + \frac{1}{r_{21}} \frac{M_2}{M_1}}\right) + \frac{M_2}{M_1}} \tag{25}$$

Note that if $r_{11} = r_{21} = r_1$ and $r_{12} = r_{22} = r_2$, eq 25 is reduced to eq 5 for the terminal model. The mole ratio of the ethylene and norbornene sites is expressed as

$$\frac{M_2^*}{M_1^*} = \frac{M_{22}^* + M_{12}^*}{M_{11}^* + M_{21}^*} = \frac{k_{111}}{k_{122}} \frac{r_{12}}{r_{11}} \frac{M_2}{M_1} \frac{\left(1 + \frac{k_{122}}{k_{222}} r_{22} \frac{M_2}{M_1}\right)}{\left(1 + r_{12} \frac{M_2}{M_1}\right)} \frac{\left(1 + \frac{1}{r_{21}} \frac{M_2}{M_1}\right)}{\left(1 + \frac{k_{112}}{k_{212}} \frac{1}{r_{21}} \frac{M_2}{M_1}\right)} \tag{26}$$

To determine the kinetic parameters in the copolymer composition equation, we use the optimal parameter estimation technique using the copolymer yield and copolymer composition data. The ethylene and norbornene homopolymerization rate constants are set as follows: $k_{111} = 1.67 \times 10^7$ (L/mol-h) and $k_{222} = 1.56 \times 10^2$ (L/mol-h). Here, we assume that r_{11} and r_{12} correspond to r_1 (=1.47) and r_2 (=0.024) in the terminal model. In other words, we assume that ethylene as a penultimate unit has little effect on the relative insertion rate of ethylene and norbornene. Thus, the kinetic parameters to be estimated are: k_{122}, k_{211}, r_{21}, r_{22}. For the optimization calculations, we use the sequential quadratic programming method in MATLAB Optimization Toolbox. In this technique, the constrained minimum of a scalar function of several variables is found through line search starting at an initial estimate. The overall scalar objective function (F) is defined as a total sum of squared errors between the data and the model predictions:

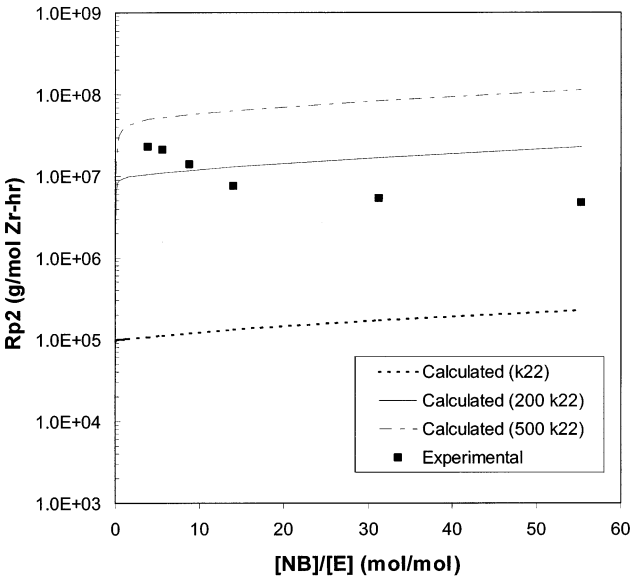

Figure 5. Norbornene polymerization rates calculated by terminal model with different values of norbornene homopolymerization rate constant (k_{22}).

$$F = \sum_i F_i = w_1(i) \left(\frac{Y_m(i) - Y_{exp}(i)}{Y_{exp}(i)}\right)^2 + w_2(i) \left(\frac{X_m(i) - X_{exp}(i)}{X_{exp}(i)}\right)^2 \tag{27}$$

where F_i = scalar objective funcition for the ith experimental data set, $w_1(i)$ = weighting factor, $Y_m(i)$ = model predicted copolymer yield, $Y_{exp}(i)$ = experimentally measured copolymer yield, $X_m(i)$ = model predicted norbornene mol % in the copolymer, and $X_{exp}(i)$ = experimentally measured norbornene mol % in the copolymer. The initial estimates of the parameters used in the optimization calculation are as follows: (k_{122}, k_{211}, r_{21}, r_{22}) = (1.56×10^2, 1.67×10^7, 1.47, 0.024).

The results of parameter estimation calculations are shown in Table 1. It is interesting to observe from Table 1 that the rate of norbornene insertion into the Zr−norbornene bond with ethylene as a penultimate unit (k_{122}) is about 472 times larger than that with norbornene as a penultimate unit (k_{222}). The reactivity ratio r_{12} value determined in this work is the same as reported by Tritto et al.[15] for the same catalyst although

Table 1. Kinetic Parameters for Ethylene−Norbornene Copolymerization at 70 °C

parameter	value[a]	parameter	value
k_{111}	1.67E7	r_{11}	1.47
k_{112}	1.14E7	r_{12}	0.024
k_{121}	3.07E6	r_{21}	0.887
k_{122}	7.37E4	r_{22}	9.0E−4
k_{211}	1.63E7	s_1	0.976
k_{212}	1.84E7	s_2	472.4
k_{221}	1.78E5		
k_{222}	1.56E2		

[a] L/mol-h.

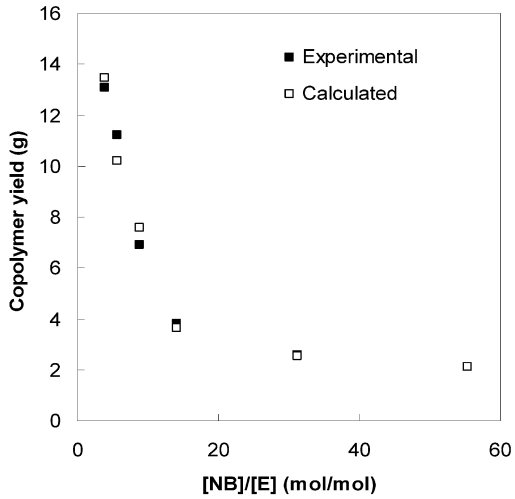

Figure 6. Copolymer yield vs bulk phase [NB]/[E] mole ratio at 70 °C: experimental data and penultimate model calculations.

their computed value of r_{11} (3.048−3.241) is larger than the value determined in this work ($r_{11} = 1.47$).

Figure 6 shows the calculated and measured copolymer yield data (10 min reaction time) for different [NB]/[E] mole ratios in the bulk phase. Notice that unlike with the terminal model calculations, the experimental copolymer yield data agree very well with the penultimate model calculations. The copolymer yields vs time plots are also shown in Figure 7. Here, for the prediction of long-term polymerization behavior, we assume the first-order site deactivation kinetics:

$$M_1^* \xrightarrow{k_{d1}} D \tag{28.1}$$

$$M_2^* \xrightarrow{k_{d2}} D \tag{28.2}$$

where D represents deactivated catalytic site. The deactivation rate constants were estimated using the optimal parameter estimation technique with experimentally measured copolymer yields vs time data. The estimated deactivation rate constants are $k_{d1} = 1.02$ min^{-1} and $k_{d2} = 0.016$ min^{-1}. Both Figures 6 and 7 show that calculated results are in excellent agreement with the experimental data. Recall that the copolymer yields predicted by the terminal model were unreasonably low (Figure 4) and the model-predicted dependence of norbornene polymerization rate on the bulk phase norbornene concentration was incorrectly predicted by the terminal model (Figure 5).

At this point, let us consider why the penultimate model yields better results than the terminal model. First, we plot the concentrations of four different types

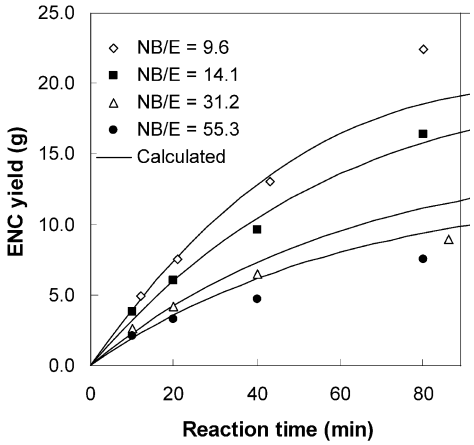

Figure 7. Copolymer yield vs reaction time at different bulk phase norbornene/ethylene mole ratios at 70 °C: symbols, experimental data; lines, penultimate model calculations.

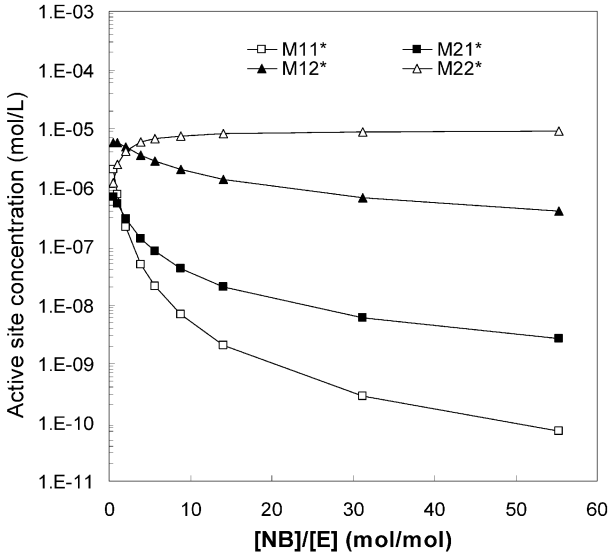

Figure 8. Active site concentrations calculated by penultimate model.

of active sites (M_{ij}^*) in Figure 8. At low [NB]/[E] mole ratios, the concentrations of these sites are quite comparable. But as the ratio is increased, the concentrations of ethylene sites (M_{11}^* and M_{21}^*) decrease dramatically and the norbornene sites with norbornene as a penultimate unit (M_{22}^*) become the dominant sites.

The individual ethylene insertion rates are also shown in Figure 9. Here, the following fractional reaction rates are defined as

$$\begin{aligned} Z_{111} &\equiv \frac{R_{p111}}{R_{p111} + R_{p211} + R_{p121} + R_{p221}}, \\ Z_{211} &\equiv \frac{R_{p211}}{R_{p111} + R_{p211} + R_{p121} + R_{p221}} \\ Z_{121} &\equiv \frac{R_{p121}}{R_{p111} + R_{p211} + R_{p121} + R_{p221}}, \\ Z_{221} &\equiv \frac{R_{p221}}{R_{p111} + R_{p211} + R_{p121} + R_{p221}} \end{aligned} \tag{29}$$

where the ethylene insertion rates are defined from eq 14:

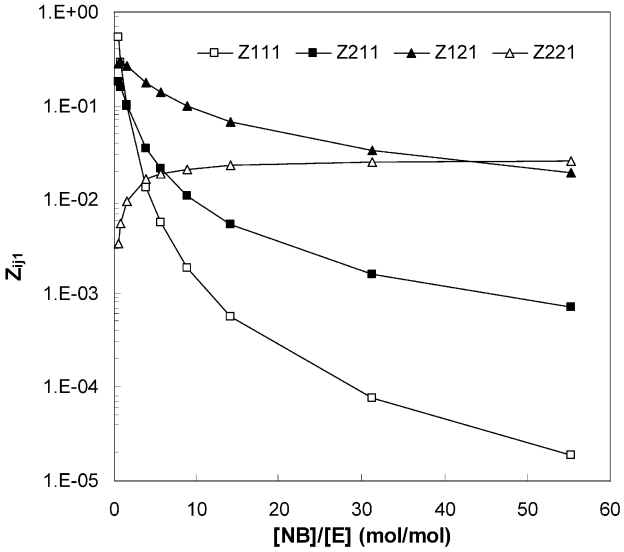

Figure 9. Effect of bulk phase [NB]/[E] mole ratio on the rates of ethylene insertion calculated by penultimate model.

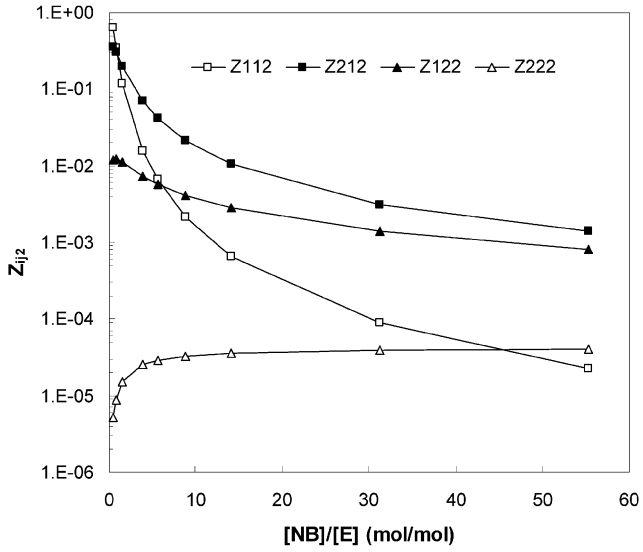

Figure 10. Effect of bulk phase [NB]/[E] mole ratio on the rates of norbornene insertion calculated by penultimate model.

$$R_{p111} = k_{111}M_{11}^{*}M_1, \quad R_{p211} = k_{211}M_{21}^{*}M_1,$$
$$R_{p121} = k_{121}M_{12}^{*}M_1, \quad R_{p221} = k_{221}M_{22}^{*}M_1 \quad (30)$$

At low [NB]/[E] mole ratios (e.g., [NB]/[E] < 5), ethylene insertion is mostly through the formation of terminal ethylene triads and diads (R_{p111}, R_{p211}) and alternating sequence (R_{p121}). However, at high [NB]/[E] mole ratios (e.g., [NB]/[E] > 5), the rates of formation of terminal ethylene triads and diads decrease significantly and ethylene is inserted as an isolated unit through R_{p221} and R_{p121} reactions.

The individual norbornene insertion rates are shown in Figure 10. Again, the following fractional reaction rates are used:

$$Z_{112} \equiv \frac{R_{p112}}{R_{p112} + R_{p212} + R_{p122} + R_{p222}},$$
$$Z_{212} \equiv \frac{R_{p212}}{R_{p112} + R_{p212} + R_{p122} + R_{p222}}$$
$$Z_{122} \equiv \frac{R_{p122}}{R_{p112} + R_{p212} + R_{p122} + R_{p222}}, \quad (31)$$
$$Z_{222} \equiv \frac{R_{p222}}{R_{p112} + R_{p212} + R_{p122} + R_{p222}}$$

where the norbornene insertion rates are defined from eq 15:

$$R_{p112} = k_{112}M_{11}^{*}M_2, \quad R_{p212} = k_{212}M_{21}^{*}M_2,$$
$$R_{p122} = k_{122}M_{12}^{*}M_2, \quad R_{p222} = k_{222}M_{22}^{*}M_2 \quad (32)$$

At low [NB]/[E] mole ratios (e.g., [NB]/[E] < 5), norbornene insertion is mostly via R_{p112} and R_{p212} reactions where the terminal unit is ethylene. However, as the [NB]/[E] mole ratio is increased, the rate of norbornene insertion into Zr−ethylene bond via R_{p112} reaction with ethylene as a penultimate unit decreases sharply. The insertion of norbornene is dominated by the formation of alternating sequence (R_{p212}) but the rate of norborne diad formation (R_{p122}) becomes relatively important. The norbornene polymerization behavior shown in Figure 10 is in contrast to the prediction by the terminal model where the insertion of norbornene is extremely slow at high [NB]/[E] mole ratios because almost all the catalyst sites are taken by norbornene and the norbornene homopolymerization rate is extremely slow.

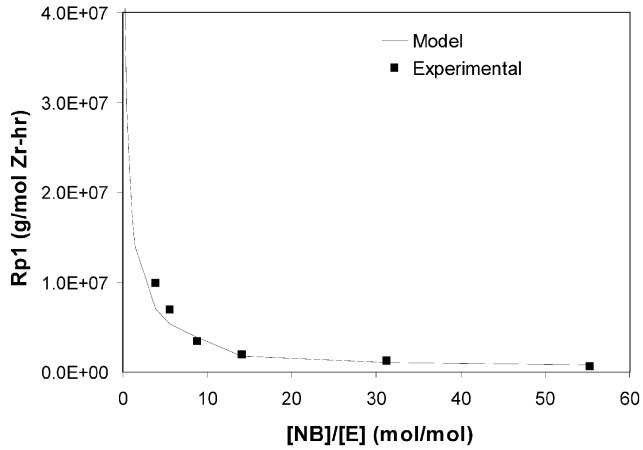

Figure 11. Effect of bulk phase [NB]/[E] mole ratio on ethylene polymerization rate (penultimated model).

The effect of bulk phase norbornene [NB]/[E] mole ratio on ethylene polymerization rate is shown in Figure 11. Here, the bulk phase ethylene concentration is held constant at 0.16 mol/L for the first three data points (model simulation: [NB]/[E] up to 8.8) and at 0.10 mol/L for the last three data points (model simulation: [NB]/[E] from 8.8 to 55.3). The experimental ethylene polymerization rate is a 10 min average of the initial polymerization rate at constant ethylene concentration. The ethylene polymerization rate decreases with an increase in norbornene concentration and the reaction rates calculated using the penultimate model are in good agreement with experimental data. Similar experimental results were reported for other metallocene catalysts.[7,20]

The penultimate model predicts an interesting kinetic behavior of ethylene−norbornene copolymerization. Figure 12 shows the experimental data and the results of penultimate model calculations of the norbornene polymerization rates for varying bulk phase [NB]/[E] mole

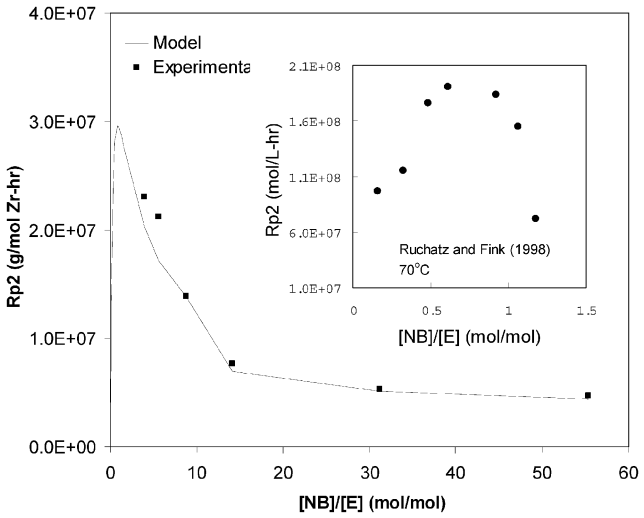

Figure 12. Effect of bulk phase [NB]/[E] mole ratio on norbornene polymerization rate (penultimated model).

ratio. Again, the bulk phase ethylene concentration is held constant at 0.16 mol/L for the first three experimental data points (model simulation: [NB]/[E] up to 8.8) and at 0.10 mol/L for the last three experimental data points (model simulation: [NB]/[E] from 8.8 to 55.3). Notice that there is a maximum in the norbornene polymerization rate. In the region of low norbornene concentrations (e.g., [NB]/[E] < 1.0 or 50 mol % norbornene), the norbornene insertion rate increases as norbornene concentration is increased. However, the norbornene insertion rate starts to decrease with a further increase in norbornene concentration. It is because at low norbornene concentrations the concentration of norbornene sites is low and the rate of norbornene polymerization increases as bulk phase norbornene concentration is increased. But at higher bulk phase norbornene concentrations (e.g., [NB] > 50 mol %), norbornene sites become dominant and steric effect causes the polymerization of norbornene to decrease as bulk phase norbornene concentration further increases. The model calculation results shown in Figures 9 and 10 indicate that the kinetics of ethylene−norbornene copolymerization at low [NB]/[E] mole ratios (e.g., [NB]/[E] < 1.0; T_g < 127 °C) is different from that at higher mole ratios.

The computational results shown in Figure 12 are in agreement with the experimental data reported by Ruchatz and Fink[7] with [(isopropylidene)(η^5-inden-1-ylidene-η^5-cyclopentadienyl)]$ZrCl_2$/MAO catalyst: they also observed a peak in norbornene polymerization rate as norbornene concentration was increased (inset in Figure 12). It is also interesting to observe that although the catalysts used are different, both our penultimate model calculations and the data by Ruchatz and Fink show that the maximum norbornene polymerization rate occurs at the [NB]/[E] mole ratio of about 0.8−1.0.

The penultimate model simulation results shown in Figure 12 are also in sharp contrast to the predictions by the terminal model: as shown in Figure 5, the terminal model fails to predict the effect of bulk phase norbornene concentration on the norbornene polymerization rate, particularly at low [NB]/[E] mole ratios. Figure 12 shows most dramatically the validity of the penultimate model proposed in this work for ethylene−norbornene copolymerization.

Conclusions

The kinetics of ethylene−norbornene copolymerization in toluene has been investigated using *rac*-Et(1-indenyl)$_2$$ZrCl_2$/MAO catalyst system at 70 °C for norbornene/ethylene mole ratios in the range 3−55. The reactivity ratios (r_1 = 1.47, r_2 = 0.024) obtained using the terminal model give a reasonably good prediction of copolymer composition; however, the terminal model fails to accurately predict the polymerization rates of ethylene and norbornene. The polymerization rates or copolymer yields calculated using the terminal model are much lower than the experimentally observed. The terminal model also gives inadequate predictions of the effect of bulk phase norbornene concentration on the norbornene polymerization rate. To overcome the limitations of the terminal model, we developed a penultimate model. The relevant kinetic parameters were estimated using experimental data and optimal parameter estimation technique. The penultimate model simulation results show that the model can very well fit the experimental data. The penultimate model calculations also indicate that the ethylene−norbornene polymerization process show different kinetic behaviors below and above the bulk phase norbornene concentration of about 50 mol %. Most importantly, unlike with the terminal model, we can correctly predict the existence of a maximum norbornene polymerization rate with the proposed penultimate model. It should be pointed out that Tritto et al.[15] also reported the validity of the second-order Markov model (penultimate model) from the microstructure analysis of ethylene−norbornene copolymers at tetrad level.

Acknowledgment. Financial support from the LG Chemical Co. is gratefully acknowledged. The authors are thankful for the ^{13}C NMR analysis by Ms. C. S. Moon.

References and Notes

(1) Kaminsky, W.; Spiehl, R. Copolymerization of cycloalkenes with ethylene in the presence of chiral zirconocene catalysts. *Macromol. Chem.* **1989**, *190*, 515−526.

(2) Kaminsky, W.; Bark, A.; Arndt, M. New polymers by homogeneous zirconocene/aluminoxane catalysts. *Makromol. Chem., Macromol. Symp.* **1991**, *47*, 83−93.

(3) Kaminsky, W.; Knoll, A. Copolymerization of norbornene and ethene with homogeneous zirconocenes/methylaluminoxane catalysts. *Polym. Bull. (Berlin)* **1993**, *31*, 175−182.

(4) Kaminsky, W. New polymers by metallocene catalysis. *Macromol. Chem. Phys.* **1996**, *197*, 3907−3945.

(5) Bergström, C. H.; Väänänen, T. L. J.; Seppälä, J. V. Effects of polymerization conditions when making norbornene-ethylene copolymers using the metallocene catalyst ethylene bis(indenyl) zirconium dichloride and MAO to obtain high glass transition temperatures. *J. Appl. Polym. Sci.* **1997**, *63*, 1063−1070.

(6) Bergström, C. H.; Väänänen, T. L. J.; Seppälä, J. V. Influence of polymerization conditions on microstructure of norbornene-ethylene copolymers made using metallocene catalysts and MAO. *J. Appl. Polym. Sci.* **1997**, *63*, 1071−1076.

(7) Ruchatz, D.; Fink, G. Ethene−norbornene copolymerization using homogeneous metallocene and half-sandwich catalysts: Kinetics and relationships between catalyst structure and polymer structure. 1. Kinetics of the ethene−norbornene copolymerization using the [(Isopropylidene)η^5-inden-1-ylidene-η^5 cyclopentadienyl] zirconium dichloride/MAO catalyst. *Macromolecules* **1998**, *31*, 4669−4673.

(8) Rische, T.; Wadden, A. J.; Dickinson, L. C.; Macknight, W. J. Microstructure and Morphology of Cycloolefin Copolymers. *Macromolecules* **1998**, *31*, 1871−1874.

(9) Provasoli, A.; Ferro, D. R.; Tritto, I.; Boggioni, L. The conformational characteristics of ethylene−norbornene co-

polymers and their influence on the ^{13}C NMR spectra. *Macromolecules* **1999**, *32*, 6697−6706.

(10) Arndt −Rosenau, M.; Beulich, L. Microstructure of ethyene−norbornene copolymers. *Macromolecules* **1999**, *32*, 7335−7343.

(11) Tritto, I.; Marestin, C.; Boggioni, L.; Zetta, L.; Provasoli, A.; Ferro, D. R. Ethylene−norbornene copolymer microstructure. Assessment and advances based on assignments of ^{13}C NMR spectra. *Macromolecules* **2000**, *33*, 8931−8944.

(12) Tritto, I.; Boggioni, L.; Jansen, J.; Thorshaug, K.; Sacchi, M. C.; Ferro, D. R. Ethylene−norbornene copolymer microstructure at tetrad level: Advances in assignments of ^{13}C NMR spectra and insights on polymerization mechanisms. Paper presented at the International Symposium on Polyolefins and Olefin Polymerization Catalysis, Tokyo, Japan, March 21−24, 2001.

(13) Forsyth, J.; Pereña, J. M.; Benavente, R.; Pérez, E.; Tritto, I.; Boggioni, L.; Brintzinger, H. H. Influence of the polymer microstructure on the thermal properties of cycloolefin copolymers with high norborene contents. *Macromol. Chem. Phys.* **2001**, *202*, 614−620.

(14) Bergström, C. H.; Sperlich, B. R.; Ruotoistenmäki, J.; Seppälä, J. V. Investigation of the microstructure of metallocene-catalyzed norbornene-ethylene copolymers using NMR spectroscopy. *J. Polym. Sci., Part A: Polym. Chem.* **1998**, *36*, 1633.

(15) Tritto, I.; Boggioni, L.; Jansen, J. C.; Thorshaug, K.; Sacchi, M. C.; Ferro, D. R. Ethylene−norbornene copolymers from metallocene-based catalysts: Microstructure at tetrad level and reactivity ratios. *Macromolecules* **2002**, *35*, 616−623.

(16) Harrington, B. A.; Crowther, D. J. Stereoregular, alternating ethylene−norbornene copolymers from monocyclopentadienyl catalysts activated with noncoordinating discrete anions. *J. Mol. Catal. A, Chem.* **1998**, *128*, 79−84.

(17) Choi, K. Y.; Park, S. Y.; Song, K. H.; Jeong, B. G. Kinetics of ethylene-cycloolefin copolymerization with *rac*-Et(Indenyl)$_2$-$ZrCl_2$/MAO catalyst system, Paper presented at the 17th International Symposium on Chemical Reaction Engineering, Hong Kong, August 25−28, 2002.

(18) Park, S. Y. A study on the kinetics of ethylene−norbornene copolymerization over homogeneous metallocene catalysts. Ph.D. Thesis, University of Maryland, College Park, MD, 2003.

(19) McKnight, A. L.; Waymouth, R. M. Ethylene/norbornene copolymerizations with titanium CpA catalysts. *Macromolecules* **1999**, *32*, 2816−2825.

(20) Herfert, N.; Montag, P.; Fink, G. Elementary processes of the Ziegler catalysis, 7. Ethylene, α-olefin and norbornene copolymerization with the sterorigid catalyst systems ^{i}Pr[FluCp]-$ZrCl_2$/MAO and $Me_2Si[Ind]_2ZrCl_2$/MAO. *Makromol. Chem.* **1993**, *194*, 3167−3182.

MA034115+